Local mechanical and dielectric behavior of the interacting polymer layer in silica nano-particles filled SBR by means of AFM-based methods

Mohammed M. Kummali [a,b], Luis A. Miccio [a,b,c,∗], Gustavo A. Schwartz [b,c], Angel Alegría [a,b], Juan Colmenero [a,b,c], Jon Otegui [c,d], Albrecht Petzold [d], Stephan Westermann [d]

[a] Departamento de Física de Materiales UPV/EHU, Fac. de Química, 20080 San Sebastián, Spain
[b] Centro de Física de Materiales CSIC-UPV/EHU, Paseo Manuel de Lardizabal 5, 20018 San Sebastián, Spain
[c] Donostia International Physics Center, Paseo Manuel de Lardizabal 4, 20018 San Sebastián, Spain
[d] Goodyear Innovation Center Luxembourg, Global Materials Science, Av. Gordon Smith, L-7750 Colmar-Berg, Luxembourg

ARTICLE INFO

ABSTRACT

Filler-polymer interactions in reinforced rubbers are mainly governed by a thin layer of polymer around the filler particles. The dynamics of this layer has long been a matter of intense investigation. Some researchers suggest that this "interacting layer" is immobilized and possesses slower dynamics compared to the bulk, whereas some others consider it equally mobile. In this work, we address this problem by studying the macroscopic characteristics of reinforced rubber using Broadband Dielectric Spectroscopy (BDS) and by measuring its local dielectric behavior using a new AFM based approach: nano-dielectric spectroscopy. This new approach enables us to study the dielectric response of the interacting polymer layer and the bulk dynamics locally, with a spatial resolution of about 20–30 nm. The total amount of interacting polymer within the compounds was also obtained by analyzing the local mechanical properties. Both macro- and nano-measurements show no differences in the polymer local dynamics for the compounds here analyzed. We propose that, for our particular system, the interacting polymer layer shares the same local relaxation dynamics with the bulk rubber due to the presence of a flexible link between the polymer chains and the nanoparticles.

1. Introduction

Styrene–butadiene–rubber (SBR) has been developed in the 1930s as a good replacement for natural rubber (NR), and rapidly became the most produced synthetic rubber. In particular, SBR for automobile tyres is usually reinforced by vulcanization and by the addition of fillers such as carbon black or silica particles. The reinforcement by activated silica filler plays an important role in improving the mechanical properties of the SBR [1–4]. One of the key factors which determine the final properties of the filled compounds is the filler–polymer interaction at the interface. Therefore, understanding the behavior of the polymer chains at this interface becomes of utmost importance in improving both, the bulk properties and the processability of these materials.

In nano-particles reinforced rubbers the existence of an immobilized polymer layer around the fillers has been a matter of debate since a long time. However, despite the intense research in this area, the polymer–filler interaction is not yet fully understood, and contradictory interpretations can be found in the literature. The problem has been mainly addressed by probing the dielectric response of reinforced rubber using Broadband Dielectric Spectroscopy (BDS) [1,5–9] along with other techniques like: Nuclear Magnetic Resonance [2,10–13] and/or Thermogravimetric Analysis (TGA) [2,14] to name a few. BDS measurements for the unfilled SBR [15] show the existence of two relaxation processes; one corresponding to the segmental (α) relaxation and the other to the secondary (β) relaxation. For nano-particles reinforced SBR an additional process is usually observed at lower frequencies. Some researchers [7–9] suggest that this relaxation is related to the immobilized polymer layer around the particles, while others [16,17] attribute this process to a Maxwell–Wagner–Sillars (MWS) polarization, arising due to the presence of trapped charges at the boundaries of the filler particles. The classical techniques so far

employed to address this problem only access the macroscopic average properties, and no information about the local behavior can be obtained.

Recent advances in atomic force microscopy allow probing locally the structural and dynamic properties of reinforced rubber. Due to its exceptionally high spatial resolution and sensitivity to mechanical forces, AFM has been widely used to study the morphology and distribution of filler within the rubber [18–21] and to probe the local mechanical properties of reinforced rubber [22,23]. In addition to the standard AFM techniques, a new approach has been recently proposed to access the local dielectric behavior: nano-dielectric spectroscopy (nDS) [24].

In this paper we probe the relaxation dynamics of the polymer layer in close proximity to the filler (the so called "interacting polymer layer") using both macroscopic and microscopic techniques. We first study the macroscopic characteristics of reinforced rubber by using Differential Scanning Calorimetry (DSC) and standard BDS. In addition, the local dielectric and mechanical behavior of the interacting polymer layer has been also studied by using nano-dielectric spectroscopy (nDS) and HarmoniX™ [25], respectively.

2. Nano-dielectric spectroscopy background

At local scale the dielectric behavior of a material can be characterized by using Electric Force Microscopy (EFM) [26–28]. In EFM, the tip–sample interaction is probed by applying an electric field to the tip. The dielectric behavior can be probed by applying either DC [29–33] or AC [34,35] electric fields. In the latter, the dielectric response of insulating films at local scale is studied by either frequency modulation (FM mode) [35,36] or amplitude modulation (AM mode) [24]. Here we use AM nDS by applying an AC signal ($V = V_0 \sin(\omega t)$) to the tip and scanning the sample using the so-called double pass method. The 2ω component of the electric force on the tip, given by $F = (1/4)(\partial C/\partial Z)v_0^2 \Box \cos\Box 2 \omega t$, contains information about the dielectric behavior of the sample through the tip–sample interaction. The tip–sample force can be related to the motion of the cantilever detected in the photodiode through the equation [24] $F = A\chi k_c$, where A is the amplitude of the photodiode signal, χ is a proportionality constant expressed in nm/V and k_c the cantilever stiffness. A Lock-In Amplifier (LIA) is used to provide the required AC signal and to filter the 2ω component of the electric force from the cantilever response. Hence, both amplitude (R) and phase (θ) of the filtered signal contain information about the local dielectric behavior of the sample. With a sharp enough tip, the lateral spatial resolution obtained with this technique is a few tens of nano-meters [37]. More details of this technique can be found elsewhere [24].

3. Experimental

3.1. Sample preparation

Samples based on commercial solution styrene-butadiene rubber BUNA VSL 5025 (SBR) were prepared. Silica nano-particles and bis(3-triethoxysilylpropyl) disulfide (TESPD) were added during the mixing process, as filler and linking agent respectively. The TESPD chemically links the nanoparticles to the rubber, thus facilitating their dispersion in the polymeric matrix. In particular, TESPD have disulfide and ethoxy reactive groups: disulfide forms a covalent bond in unsaturated rubbers like SBR, while ethoxy reacts with the silanol groups present on the surface of nanoparticles. As a result, stable covalent filler–TESPD-SBR bonds are obtained.

Two series of materials were prepared by using different silica fillers, i.e. precipitated amorphous silica 1200 MP (A) and 1165 MP (B) (Rhodia, specific surface areas of 213.1 m^2/g and 165.8 m^2/g,

respectively). In both series, filler concentrations of 30 and 90 phr (parts in weight per hundred parts of rubber) were employed. Once the compounds were mixed, square sheets were obtained by compression-molding vulcanization at 170 °C during 10 min in a mold, yielding samples of 15 × 15 cm and thickness of about 0.7 mm. From these sheets samples for DSC and BDS were obtained. Samples required for AFM measurements were cut using a cryomicrotome. In this way we ensure that at the filler surface only those polymer layers which are strongly attached to the nanoparticles, interacting layer, remains and the rest is peeled off. Sample thickness thus obtained was ca 200 nm.

3.2. Differential Scanning Calorimetry (DSC)

DSC measurements were performed using a DSC Q2000 from TA Instruments. Samples of about 10 mg were sealed in hermetic aluminum pans. Heating–cooling cycles were performed under nitrogen flow in the temperature range from −125 to 50 °C, with a heating/cooling rate of 10 °C/min. The annealing time between cooling and heating runs was 5 min. Glass transition temperature (T_g) was determined at the inflection point of the curves and the heat capacity increment (ΔCp) was estimated from the difference in height of the extrapolation of the heat capacity curve after and before the T_g at the inflection point.

3.3. Standard Broadband Dielectric Spectroscopy (BDS)

Broadband dielectric spectroscopic measurements were performed on disc shaped samples with a diameter of 40 mm and a thickness of about 0.7 mm. The samples were placed in between two parallel plate electrodes. For parallel-plate configuration, the sample capacitance is expressed as $C = \varepsilon\, \varepsilon_0\, A/d$, where ε is the relative dielectric permittivity of the sample, ε_0 is the vacuum permittivity, A is the section of the sample, and d its thickness. The material properties are characterized by the complex dielectric permittivity, ε^*, which is defined as $\varepsilon^*(\omega) = C^*(\omega)/C_0 = \varepsilon'(\omega) - i\,\varepsilon''(\omega)$, where C_0 is the capacitance of the empty capacitor and $\omega = 2\pi f$. Broadband high-resolution dielectric spectrometer (Novocontrol Alpha analyser) was used to measure the complex dielectric permittivity in the frequency range from 10^{-2}–10^6 Hz. Isothermal frequency scans were performed every third degree over the temperature range 253–353 K. The sample temperature was controlled by a nitrogen gas flow that provides temperature stability of about ±0.1 K.

3.4. Nano-dielectric spectroscopy (nDS)

Topography and mechanical phase images of the samples were recorded simultaneously using standard tapping mode, in order to identify the nano-particle clusters and the bulk-like areas. nDS was then performed by applying a sinusoidal voltage to the tip in lift mode (double pass method), and analyzing the cantilever motion signal with an external LIA (Stanford Research SR830). The conductive cantilevers used for the measurements were Antimony (Sb) doped Si, coated with Pt/Ir (SCM − PIT tips, Bruker). The nominal values for the natural frequency, tip radius, and cantilever spring constant were 75 kHz, 20 nm and 1.5–3 N/m respectively. With this configuration, the lateral spatial resolution of the technique is about 20–30 nm [37]. For each electrical excitation frequency applied to the tip, the phase of the cantilever response at 2ω is recorded. Additionally, before measuring the sample response, a reference experiment is performed on a gold substrate. Therefore, the dielectric spectra are obtained by plotting the difference between sample and reference as a function of frequency [24]. The measurements were performed for temperatures ranging

from −10−100 °C, by using a Peltier cooler/heater with a silicone cap used as sealing. The temperature was set and controlled by using a Thermal Applications Controller (TAC, Bruker).

3.5. Single pass EFM (SP-EFM) imaging

In single pass EFM imaging, both the topography and dielectric contrast response of the sample are obtained during the main scan itself [38]. The phase of the cantilever signal obtained from the LIA (at a frequency double than the electric excitation frequency) is mapped along with the topography and the mechanical phase. In this way we simultaneously image the topographical features and dielectric contrast map of the sample.

3.6. HarmoniX™

Mechanical characterization of the samples at nano-scale was performed using HarmoniX™ AFM imaging [25,39,40]. HarmoniX™ measurements were conducted in air under ambient condition using a Multimode 8 AFM (Bruker). HarmoniX™ can provide simultaneous information about various mechanical properties of the sample like: modulus, surface adhesion or elasticity, to name a few. For HarmoniX™ measurements, specifically designed torsional harmonic cantilevers were employed (HMX−10, Bruker). The nominal values for the natural frequency, tip radius and cantilever spring constant for these probes were 70 kHz, 10 nm and 1.5−6 N/m respectively. The measurements were performed in moderate/hard tapping mode ($A_{sp}/A_0 = 0.6/0.5$, where A_{sp} is the set point amplitude and A_0 is the free oscillation amplitude).

4. Results and discussion

4.1. Macroscopic characterization

DSC and BDS were employed for the macroscopic characterization of the materials. While calorimetric data renders information about temperatures and heat flows associated with thermal transitions within the whole sample, dielectric data yields information of those polymer segments having a dielectric response within a given frequency/temperature range.

4.1.1. DSC measurements

Fig. 1 shows heat flow plotted as a function of temperature for the unfilled, 30 phr silica B and 90 phr silica B samples. The figure
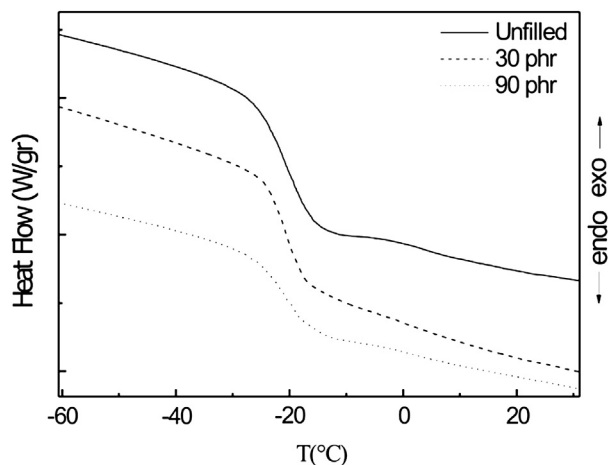
shows the same glass transition temperature (252 ± 0.2 K for the unfilled, 252.4 ± 0.3 K for 30 phr and 252.4 ± 0.4 K for 90 phr) for all the samples, independent of their filler content. Furthermore, neither a second glass transition nor significant broadening was detected. Nevertheless, a decrease in the heat capacity increment (ΔCp) at T_g is observed as the filler content increases. ΔCp values of the unfilled, 30 phr and 90 phr silica filled samples are 0.394 ± 0.012 J g^{-1} °C^{-1}, 0.301 ± 0.016 J g^{-1} °C^{-1}, and 0.192 ± 0.016 J g^{-1} °C^{-1}, respectively. This decrease in ΔCp arises from the lower amount of polymer in the samples as the filler content increases. The obtained results are the same for both material series (silica A and B), and are also consistent with earlier studies [5,41] performed on similar systems.

4.1.2. BDS measurements

Fig. 2.1 shows dielectric loss spectra (ε'' vs. frequency) obtained by standard BDS for silica (A) filled SBR with 0, 30 and 90 phr at 298 K. At this temperature, the α-relaxation of the polymer appears at around 10^5 Hz and the conductivity contribution is detected as an increase in the signal at low frequencies (see unfilled sample). In addition, a third process appears at intermediate frequencies for the filled samples. Although the origin of this process is still under debate, recent studies show that this relaxation is compatible with an MWS relaxation [16]. This process arises from the movement of trapped charges at the polymer−nanoparticle interface and therefore, its contribution increases as the filler content increases. The MWS process disappears from the experimental window after drying the samples under vacuum, as shown in Fig. 2.2. The obtained results agree with earlier studies performed on similar
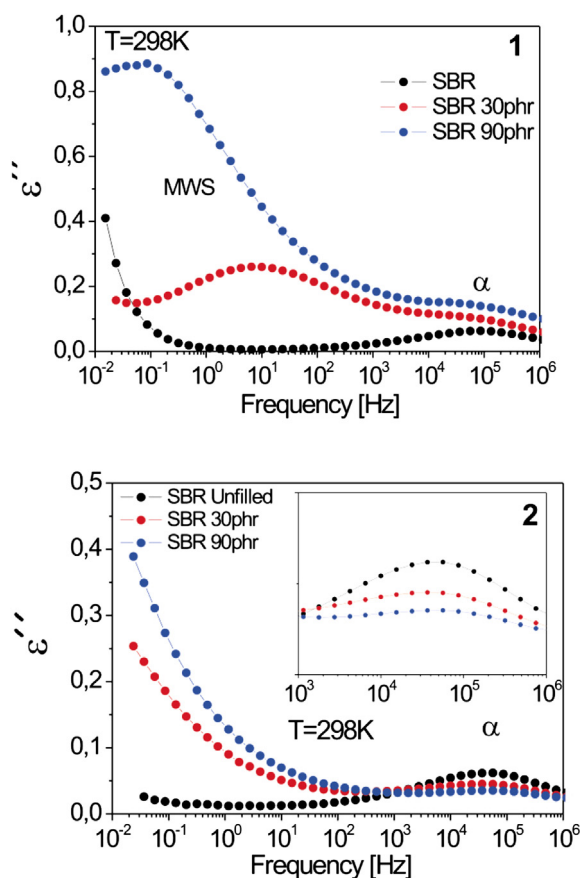
Fig. 2. Dielectric loss spectra at a fixed temperature (298 K) for unfilled SBR (●), 30 phr filled SBR (●) and 90 phr filled SBR (●) (Silica A). 1) As received samples. 2) Vacuum dried samples (inset shows a zoomed view of α process).

Fig. 1. DSC of unfilled, 30 and 90 phr silica (B) filled SBR samples measured at a heating rate of 10 °C/min (for clarity purposes a vertical shift was applied to the curves).

systems [41]. A more detailed analysis about the MWS process dependence on the drying and rehydrating processes can be found in reference 14.

Concerning the α-relaxation, we could not observe any shift in the position of the peak maximum for this process with varying filler contents (see inset in Fig. 2.2). The fact that there is no significant change in the α-relaxation dynamics between unfilled, 30 phr and 90 phr samples suggests that either the interacting polymer layers exhibit similar segmental relaxation dynamics as that of the bulk rubber, or that the contributions to the macroscopic signal of this polymer layer is negligible. In order to elucidate this point we performed a local characterization of the interacting layer by means of AFM based methods.

4.2. Local characterization

4.2.1. nDS measurements

As it was explained above, nDS measurements are based on a double pass AFM method: in the first pass the standard tapping imaging is performed while in the second one (performed at a constant height over the sample surface) the frequency dependent electrical response is detected through the analysis of the cantilever oscillation. The measurements were performed at specific locations selected from previously obtained AFM topography images, using very small tip—sample distances (of about 5 nm).

Given the possibility of having different segmental dynamics close to the silica nanoparticles, nano-dielectric spectroscopy could provide some insight into this issue. By measuring in 1) a nanoparticle-rich location of the material and 2) a nanoparticle-free location (bulk like polymer), differences in the interacting layer contribution to the response signal could be detected. In this way, both MWS and α-relaxation processes could reveal information of the local dynamics of the polymer.

4.2.2. Unfilled rubber

As a first step, the local dielectric response of the bulk polymer was obtained from the unfilled sample. In this case, AFM images were completely homogenous due to the absence of nanoparticles (images not shown). In this sample, any detected dielectric response should come entirely from bulk polymer chains. Furthermore, as no interfaces are present, α-relaxation should be the only detectable process in our experimental frequency window. nDS measurements were performed at different points of the samples, at temperatures ranging from −10−27 °C. The obtained peaks are closely related to the macroscopic dielectric losses and, as expected, no interfacial polarization effects were observed, as shown in Fig. 3.

The inset in Fig. 3 shows the relaxation times (calculated as the reciprocal of the angular frequency at the peak maximum) obtained by both nDS and standard BDS techniques. As expected, nDS data follows the macroscopic behavior [42].

4.2.3. Filled rubber

As a second step, we studied the local dielectric response of the filled samples. Fig. 4 shows AFM (mechanical) phase images for 30 phr silica (A) filled SBR sample. The gray circles denote typical locations at which nano-dielectric measurements were performed.

In order to gain some insight into the dielectric properties of the interacting layer, both MWS and α-relaxation processes were studied at different locations. Therefore, observed differences in their local dielectric response will be related with changes in the local dielectric properties of the materials.

Fig. 5 shows nDS spectra acquired at different locations on the sample. The signals obtained above locations with elevated concentration of nanoparticles presented higher intensity than the ones obtained above bulk like locations. After drying the samples
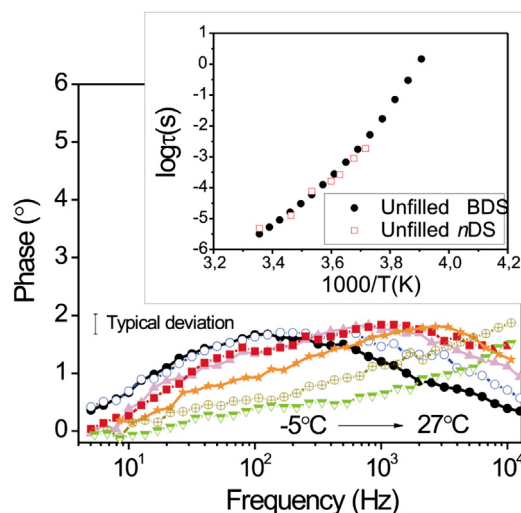
Fig. 3. nDS dielectric response spectra for unfilled SBR at different temperatures (from left to right: −5, −3, 0, 5, 10, 15 and 27 °C). Inset: nDS and BDS obtained relaxation map.

24 h at 100 °C under vacuum, this process is shifted to lower frequencies (see Fig. 4 in Ref. [16]). Furthermore, as the sample is progressively rehydrated, it recovers the previous frequency dependence (see inset in Fig. 5), in agreement with recent macroscopic studies [16,43]. According to all these results, it is most likely that the observed process corresponds to the MWS relaxation observed by BDS (see Fig. 2). As stated before, the MWS arises from the motion of trapped charges at the filler-polymer interface; therefore, the observed small tendency (a systematic higher intensity in the more concentrated locations) might originate from the increasing amount of interface within the probe volume.

Concerning the α-relaxation process, no detectable changes in the nDS spectra of the samples were observed (not shown). Therefore, the possible existence of differences in the α-relaxation was further studied by using single pass EFM imaging. This method provides an enhanced dielectric contrast image compared to double pass imaging [43]. In this case, the polymer dynamics was mapped simultaneously with sample topography. Both frequency and temperature were selected so as to match the α-relaxation timescale of the bulk polymer, obtained from unfilled experiments (see Fig. 3), within the experimental window. Therefore, any difference in the dynamics should be reflected as a change in the
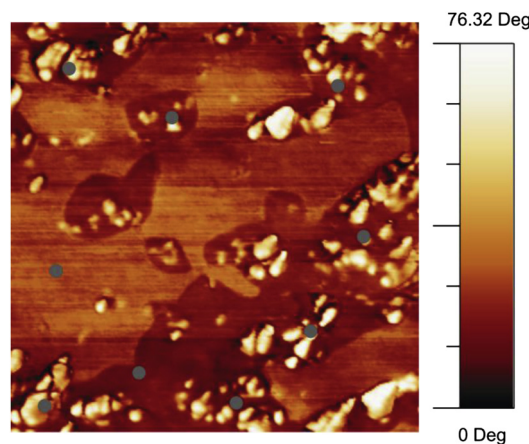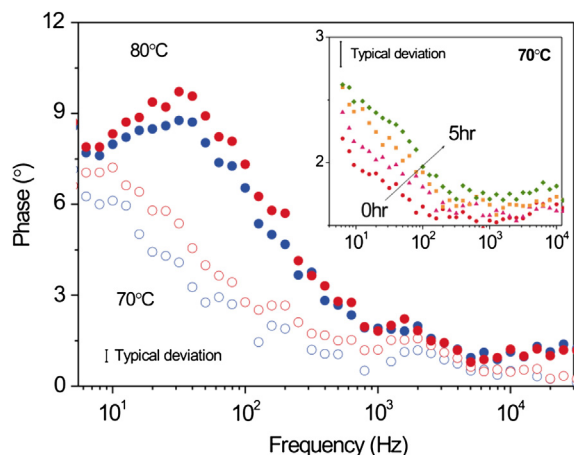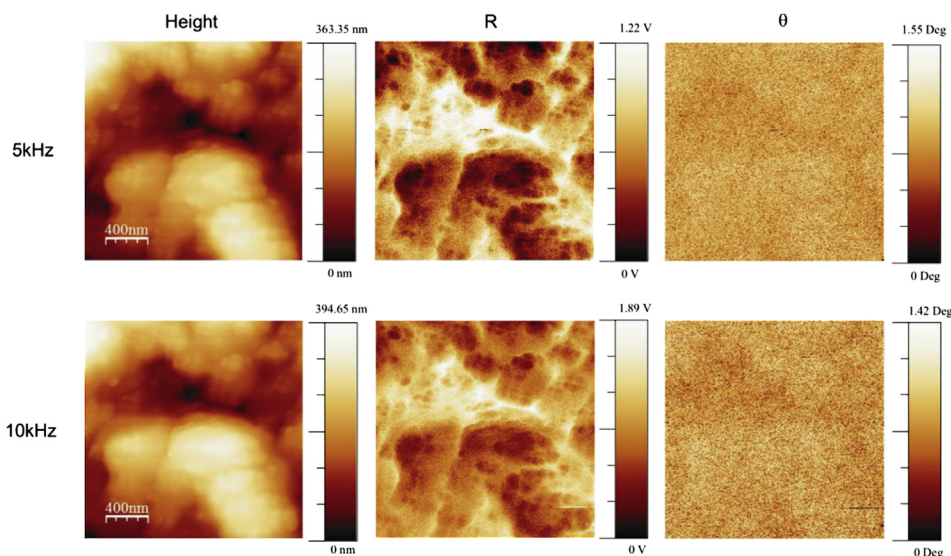
Fig. 4. Tapping phase image for the 30 phr silica (A) filled SBR sample (1 μm × 1 μm). The gray circles denote typical points at which nano-dielectric measurements were performed.

Fig. 5. *n*DS spectra of 30 phr Silica (B) filled SBR. Open circles: 70 °C. Filled circles: 80 °C. Red and blue symbols represent measurements over regions with high and low nano-particles concentration, respectively. Inset: *n*DS spectra acquired at different times after drying the sample 24 h at 100 °C under vacuum. In order to observe the rehydration effect on the spectra, the sample was maintained at 70 °C and open to the environmental humidity (no nitrogen flow inside the silicone cap). (For interpretation of the references to color in this figure legend, the reader is referred to the web version of this article.)

image contrast [44]. Fig. 6 shows topography, *R* and *θ* images at 25 °C and different excitation frequencies. The oscillation amplitude signal (*R*) reveals the presence of the nanoparticles as dark locations dispersed in a brighter polymer matrix. This contrast arises from differences between the dielectric permittivity of the silica and the rubber. The dielectric phase (*θ*) signal, which reflects the dielectric losses of the material, does not show significant contrast near nor far from the nanoparticles in the analyzed frequency range (slightly darker areas are related to the influence of large topography features on dielectric measurements). Furthermore, by comparing the images at 5 and 10 kHz it is possible to conclude that no appreciable changes in the behavior of polymer-rich/nanoparticle-rich locations are observed. These results suggest that either the dielectric losses along the different locations are the same, or that the signal coming from the interacting layer is negligible.

4.2.4. Interacting rubber

In order to gain some insight on the relevance of the interacting rubber contribution to the overall dielectric signal, a calculation of the interacting/bulk polymer ratio becomes necessary. Therefore, we employed local mechanical measurements to estimate the interacting rubber thickness, and consequently, its concentration.

AFM operating in HarmoniX™ mode provides information about different mechanical properties of the sample with high lateral resolution in a single scan. Four different signals viz. topography, phase, modulus and energy dissipation of 30 phr silica (A) filled SBR are shown in Fig. 7. The size of these aggregates varies between 80 and 120 nm. In Fig. 7, brighter regions in the phase image correspond to silica particles richer areas. Since these areas are stiffer (due to the substrate effect) in comparison to the bulk-like rubber, they have higher modulus (as is evident from the modulus image). Dissipation corresponds to the energy loss of the probe due to tip−sample interactions, and therefore stiff regions are expected to have lower dissipation than soft ones. The measurements are in agreement with earlier studies for other nano-particle reinforced rubbers analyzed using HarmoniX™ [22].

4.2.4.1. Polymer on the surface of the nanoparticles.
Fig. 7 (bottom-left) shows non-zero energy dissipation over the nanoparticles richer areas. This implies that there is a significant amount of polymer over these surfaces, which is responsible for the energy dissipation. Therefore, the polymer over the particles appears in dark-brown, while the bulk-like rubber appears in light yellow. The contrast for the polymer layer above and around the particles is most likely produced by the substrate effect. Fig. 8 gives a detailed illustration of topography and dissipation of the same sample, along with a scheme (see Fig. 8(3)) of the thickness of the polymer layer around the nanoparticles. HMX force curves obtained at small oscillation amplitudes yielded indentation depths of about 1−2 nm. According to literature [46], in order to neglect substrate effects affecting the mechanical properties, the indentation depth should be lower than about 20% of the thickness. Therefore, as we are detecting changes in the mechanical properties with these indentation depths, the layer thickness should be smaller than 5 nm for area A, and even thinner for B and C (see Fig. 8(3)). This result is in close agreement with the thickness of the interacting polymer layers previously reported in the literature [6,47].
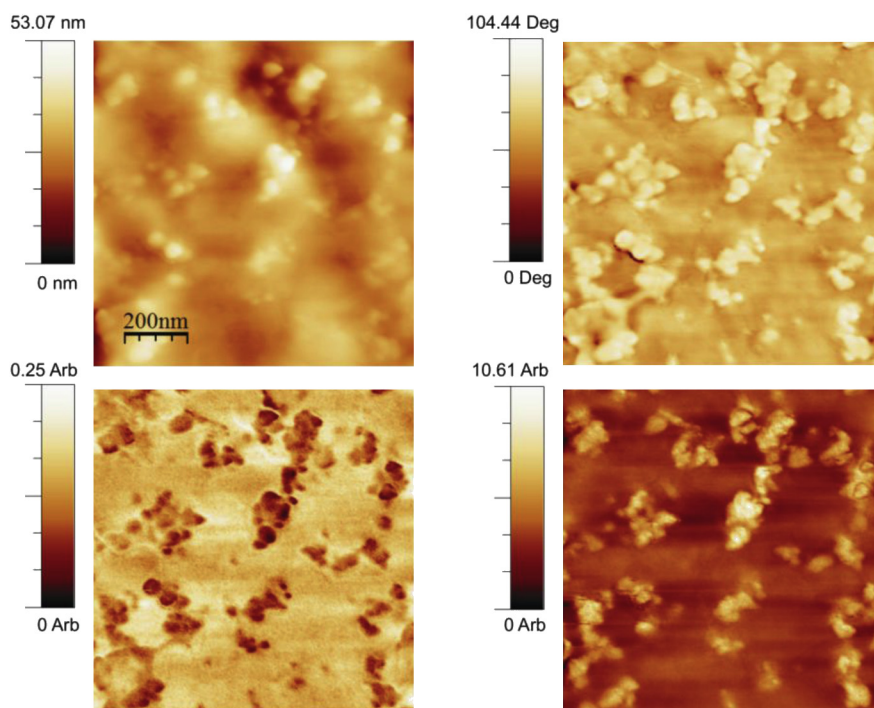

Fig. 6. Topography, *R* (dielectric oscillation amplitude) and *θ* (dielectric phase) images of 30 phr silica (B) filled SBR obtained through SP-EFM imaging during the same measurement. The experiments were performed at 25 °C using 5 and 10 kHz as electrical excitation frequencies. Both temperature and excitation frequencies were selected from unfilled α-relaxation shown in Fig. 3.

Fig. 7. (Clock wise from top left) Topography, Phase, DMT modulus and energy dissipation for 30 phr silica (A) filled sample. Images were processed using WSxM [45].
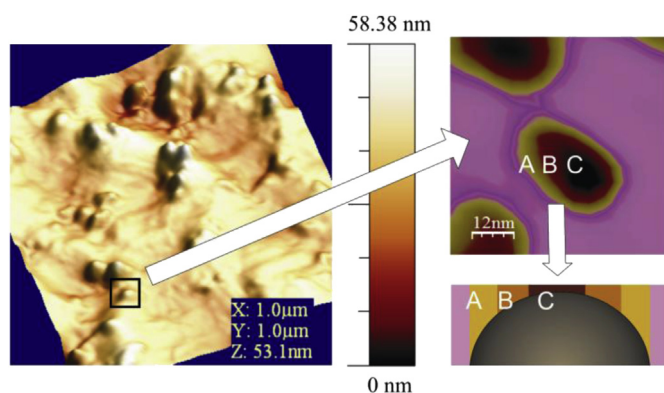

Fig. 8. Topography (1), energy dissipation for a zoomed area (2) and scheme of a sectional cut of the sample (3).
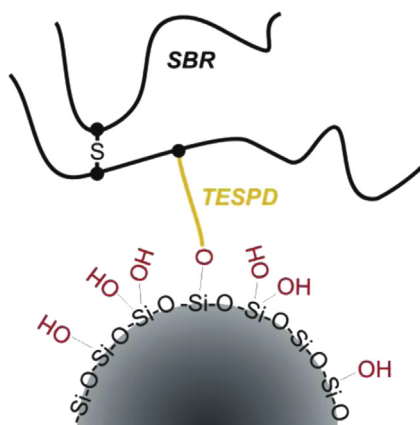

Fig. 9. Schematic representation of the TESPD mediated filler–polymer interaction.

4.2.4.2. Interacting rubber concentration. Based on previous results [6,47,48] and according to our measurements (explained above), we can assume a thickness for the interacting rubber layer ranging from 1 to 5 nm. Therefore, by considering a homogeneous distribution of nanoparticles throughout the material it is possible to calculate (for a 30 phr sample) a total concentration of interacting rubber ranging from 6 to 39%, respectively. It is worth stressing that the calculation does not consider clustering of nanoparticles, therefore, real concentration values would be slightly lower.

Despite of this non-negligible amount of interacting rubber we could not observe differences in the α-relaxation process (neither by BDS nor by DSC). In addition, no local differences in the dielectric losses were observed by nDS. These results could be rationalized by considering that the segmental dynamics of the interacting layer is not strongly affected by the presence of the filler and therefore it is rather similar to that of the bulk-like rubber. The chemistry of these materials may possibly shed some light on this matter. Fig. 9 shows a schematic representation of the TESPD mediated filler-polymer interaction. For silica-TESPD-SBR compounds, the interacting polymer layer is chemically bounded to the particles through flexible links, which in turn allows it to have a bulk like segmental dynamics. This particular kind of filler-polymer interaction does not present significant (if any) amount of immobilized polymer at the nanoparticles surfaces.

5. Conclusion

Silica nanoparticles filled SBR compounds with different filler concentration were analyzed by means of DSC, BDS, Harmonix™ and nano-dielectric spectroscopy. The nano-mechanical characterization of the filled samples revealed the presence of a thin interacting layer over the nanoparticles, surrounded by bulk like polymer. The interacting polymer layers are sometimes referred to as immobilized, and assumed to display slower segmental relaxation than the bulk. We probed the dielectric response of these layers both locally and macroscopically. Despite the relative big amount of interacting rubber

present in the materials, no such slower segmental dynamics was observed in any case. As a result, we consider that the interacting polymer layer share the same segmental relaxation dynamics with the bulk rubber, due to the presence of a flexible chain between the matrix and the nanoparticles.

Acknowledgments

References

[1] Robertson CG, Roland CM. Rubber Chem Technol 2008;81(3):506—22.
[2] Yatsuyanagi F, Suzuki N, Ito M, Kaidou H. Polymer 2001;42(23):9523—9.
[3] Luo H, Klüppel M, Schneider H. Macromolecules 2004;37(21):8000—9.
[4] Meier JG, Fritzsche J, Guy L, Bomal Y, Klüppel M. Macromolecules 2009;42(6): 2127—34.
[5] Fragiadakis D, Bokobza L, Pissis P. Polymer 2011;52(14):3175—82.
[6] Harton SE, Kumar SK, Yang HC, Koga T, Hicks K, Lee E, et al. Macromolecules 2010;43(7):3415—21.
[7] Hernandez M, Carretero-Gonzalez J, Verdejo R, Ezquerra TA, Lopez-Manchado MA. Macromolecules 2010;43(2):643—51.
[8] Kluppel M. J Phys — Condens Matter 2009;21(3):035104.
[9] Vo LT, Anastasiadis SH, Giannelis EP. Macromolecules 2011;44(15):6162—71.
[10] Arantes TM, Leao KV, Tavares MIB, Ferreira AG, Longo E, Camargo ER. Polym Test 2009;28(5):490—4.
[11] Berriot J, Lequeux F, Monnerie L, Montes H, Long D, Sotta P. J Non-Cryst Solids 2002;307:719—24.
[12] Dutta NK, Choudhury NR, Haidar B, Vidal A, Donnet JB, Delmotte L, et al. Polymer 1994;35(20):4293—9.
[13] Tsagaropoulos G, Eisenberg A. Macromolecules 1995;28(1):396—8.
[14] Pal K, Pal SK, Das CK, Kim JK. Tribol Int 2010;43(8):1542—50.
[15] Cerveny S, Bergman R, Schwartz GA, Jacobsson P. Macromolecules 2002;35(11):4337—42.
[16] Otegui J, Schwartz GA, Cerveny S, Colmenero J, Loichen J, Westermann S. Macromolecules 2013;46:2407—16.
[17] Schonhals A, Goering H, Costa FR, Wagenknecht U, Heinrich G. Macromolecules 2009;42(12):4165—74.
[18] Johnson LL. Rubber Chem Technol 2008;81(3):359—83.
[19] Mele P, Marceau S, Brown D, de Puydt Y, Alberola ND. Polymer 2002;43(20): 5577—86.
[20] Niedermeier W, Raab H, Maier P, Kreitmeier S, Goritz D. Kautschuk Gummi Kunststoffe 1995;48(9):611.
[21] Sadhu S, Bhowmick A. J Mater Sci 2005;40(7):1633—42.
[22] Schon P, Dutta S, Shirazi M, Noordermeer J, Vancso GJ. J Mater Sci 2011;46(10):3507—16.
[23] Shanmugharaj AM, Ray S, Bandyopadhyay S, Bhowmick AK. J Adhes Sci Technol 2003;17(9):1167—86.
[24] Schwartz GA, Riedel C, Arinero R, Tordjeman P, Alegria A, Colmenero J. Ultramicroscopy 2011;111(8):1366—9.
[25] Sahin O, Magonov S, Su C, Quate CF, Solgaard O. Nat Nanotechnol 2007;2(8): 507—14.
[26] Girard P. Nanotechnology 2001;12(4):485—90.
[27] Martin Y, Abraham DW, Wickramasinghe HK. App Phys Lett 1988;52(13): 1103—5.
[28] Lanyi S, Torok J, Rehurek P. J Vac Sci Technol B 1996;14(2):892—6.
[29] Riedel C, Arinero R, Tordjeman P, Leveque G, Schwartz GA, Alegria A, et al. Phys Rev E 2010;81(1):010801.
[30] Krayev AV, Talroze RV. Polymer 2004;45(24):8195—200.
[31] Miccio LA, Kummali MM, Montemartini PE, Oyanguren PA, Schwartz GA, Alegria A, et al. J Chem Phys 2011;135(6):064704.
[32] Riedel C, Arinero R, Tordjeman P, Ramonda M, Leveque G, Schwartz GA, et al. J Appl Phys 2009;106(2):024315.
[33] Kummali MM, Schwartz GA, Alegria A, Arinero R, Colmenero J. J Pol Sci Pol Phys 2011;49(18):1332—8.
[34] Crider PS, Majewski MR, Zhang J, Oukris H, Israeloff NE. App Phys Lett 2007;91(1):013102.
[35] Riedel C, Sweeney R, Israeloff NE, Arinero R, Schwartz GA, Alegria A, et al. App Phys Lett 2010;96(21):213110.
[36] Nguyen HK, Prevosto D, Labardi M, Capaccioli S, Lucchesi M, Rolla P. Macromolecules 2011;44(16):6588—93.
[37] Riedel C, Alegria A, Schwartz GA, Colmenero J, Saenz JJ. Nanotechnology 2011;22(28):285705.
[38] Magonov S, Alexander J. Beilstein J Nanotechnol 2011;2:15—27.
[39] Sahin O. Rev Sci Instrum 2007;78:103707.
[40] Sahin O, Erina N. Nanotechnology 2008;19:445717.
[41] Robertson CG, Rackaitis M. Macromolecules 2011;44(5):1177—81.
[42] Nguyen HK, Labardi M, Capaccioli S, Lucchesi M, Rolla P, Prevosto D. Macromolecules 2012;45(4):2138—44.
[43] Cerveny S, Schwartz GA, Otegui J, Colmenero J, Loichen J, Westermann S. J Phys Chem C 2012;116(45):24340—9.
[44] Kummali MM, Schwartz GA, Alegria A, Colmenero J. Imaging Microsc 2012;1: 43—5.
[45] Horcas I, Fernandez R, Gomez-Rodriguez JM, Colchero J, Gomez-Herrero J, Baro AM. Rev Sci Instrum 2007;78(1):013705.
[46] Saha R, Nix WD. Acta Materialia 2002;50(1):23—38.
[47] Glomann T, Schneider GJ, Allgaier J, Radulescu A, Lohstroh W, Farago B, et al. Phys Rev Lett 2013;110:178001.
[48] Papon A, Montes H, Hanafi M, Lequeux F, Guy L, Saalwächter K. Phys Rev Lett 2012;108(6):065702.